Original Article
A promising way to enhance *in vitro* expansion of adipose-derived stem cells

Tingliang Wang, Yi Zhang, Ying Liu, Hua Xu, Jiasheng Dong

Department of Plastic and Reconstructive Surgery, Shanghai Ninth People's Hospital Affiliated to Shanghai Jiao Tong University School of Medicine, Shanghai, China

Abstract: Adipose-derived stem cells (ASCs) are one of the most promising therapeutic cells for cell-based regenerative medicine. The applications include bone regeneration, cartilage repair, nerve regeneration, muscle and cardiac muscle repair, and liver regeneration. However, *in vitro* expansion is a crucial step before application. One of the most significant drawbacks of ASCs and all other mesenchymal stem cells is cellular aging during *in vitro* expansion. However, the extracellular matrix (ECM), which has a profound effect on cell function, offers a potential method to solve this problem. In this study, both ASCs and dermal fibroblasts (DFBs) were used to coat culture flasks with decellularized ECM (dECM). Then, ASCs were expanded on ASCs-derived dECM (AECM), DFBs-derived dECM (DECM), and conventional plastic flasks (PLs) for further proliferation and differentiation assays. Both the AECM and DECM could significantly facilitate proliferation of ASCs. ASCs expanded on AECM exhibited higher differentiation potential for osteogenesis, adipogenesis, and chondrogenesis than those expanded on DECM and PLs. The results demonstrate that AECM can successfully enhance the self-renewal and differentiation potential of ASCs, which could be a promising method for *in vitro* cell expansion in ASCs-based regenerative medicine.

Keywords: Adipose-derived stem cells, decellularized extracellular matrix, cell expansion, proliferation, differentiation

Introduction

Adipose-derived stem cells (ASCs) are one of the most promising adult mesenchymal stem cells (MSCs) for regenerative medicine [1]. Large amounts of human adipose tissue can be easily obtained with little donor site morbidity through the convenient procedure of liposuction [2]. Furthermore, ASCs have been shown to have the potential to differentiate along not only mesodermal lineages but also ectodermal and endodermal lineages [2-4]. Although the use of ASCs for clinical trials has achieved remarkable progress, some common challenges remain unsolved [5]. It is now believed that MSCs have special niches that accommodate them and provide a microenvironment to maintain stemness *in vivo* [6]. However, for all MSCs, *ex vivo* expansion without the particular niches is a required step to obtain a sufficient amount of therapeutic cells before application. Nonetheless, optimum conditions for cell expansion in which MSCs do not lose their proliferative and differentiation capacity quickly have yet to be established [7, 8].

Decellularized extracellular matrix (dECM) could imitate the *in vivo* niches by retaining similar structure and composition [6, 9, 10]. There are two ways to obtain dECM: *in vivo* tissue decellularization and *in vitro* cell culture fabrication. The latter can provide a standardized dECM product for cell expansion and has the potential for large-scale industrial manufacture. Previous studies have demonstrated that dECM from *in vitro* cell culture fabrication has a rejuvenating effect on MSCs by enhancing self-renewal and chondrogenic potential [11, 12]. However, not all dECMs exhibit the same effect and each type displays different properties based on species, donor age, and source of tissues [13]. To the best of our knowledge, no study has focused on the rejuvenating effect of ASCs-derived dECM on ASCs expansion *in vitro*.

In the current study, it was hypothesized that dECM deposited by ASCs could better facilitate

self-renewal and the differentiation potential of ASCs than that deposited by non-MSCs including fibroblasts. ASCs were evaluated by proliferation rate, stemness genes, MSC surface phenotype, and chondrogenic, adipogenic, and osteogenic potentials after cell expansion on conventional plastic flasks (PLs), dermal fibroblasts (DFBs)-derived dECM (DECM), and ASCs-derived dECM (AECM).

Materials and methods

Cell culture

Human adipose tissue was harvested from four female donors (average age, 32 years) by liposuction following approval from the Ethics Committee of Shanghai Jiaotong University School of Medicine and informed written consent was provided by the patients. After harvesting, the adipose tissue was minced into smaller pieces and digested by 2 mg/ml collagenase (NB4 [PZ activity, 0.17 U/mg]; SERVA Electrophoresis, Heidelberg, Germany) for 120 minutes in a 37°C shaking water bath. Then, the samples were filtered, centrifuged, and washed once with phosphate-buffered saline (PBS). After that, the cells were seeded on T175 culture flasks at a density of 6,000/cm^2 in α-minimum essential medium containing 10% fetal bovine serum, 100 U/ml penicillin, 100 µg/ml streptomycin, and 0.25 µg/ml fungizone (all from Invitrogen, Carlsbad, CA, USA) in a 37°C humidified incubator with 5% CO_2. The growth medium was changed every 2-3 days until cells were 80% confluent. Then, the ASCs were detached and seeded at a density of 3,000/cm^2 for expansion.

Skin samples were harvested from routine circumcision of four patients (average age, 19 years) following approval from the Ethics Committee of Shanghai Jiaotong University School of Medicine. Informed written consent was provided by the patients or their guardians. Each skin specimen was depleted of subcutaneous tissue and cut into 1-cm × 1-cm pieces before incubated in 8 U/ml dispase (Worthington Biochemical, Lakewood, NJ, USA) at 4°C overnight. The epidermis was separated from the dermis with forceps. Then, the dermis was minced into pieces and digested in 2 mg/ml collagenase (NB4, SERVA Electrophoresis) for 3 hours in a 37°C shaking water bath. Next, the samples were filtered, centrifuged, and washed

once with PBS. After that, the cells were seeded on T175 flasks at a density of 6,000/cm^2 in growth medium in a 37°C humidified incubator with 5% CO_2. The growth medium was changed every 2-3 days until cells were 80% confluent. Finally, the DFBs were detached and seeded at a density of 3,000/cm^2 for expansion.

dECM preparation

Both ASCs and DFBs were used to prepare dECM, termed AECM and DECM, respectively. The protocol followed was described previously [12, 14, 15]. Briefly, PLs were pre-coated with 0.2% gelatin for 1 hour at 37°C and seeded with passage 3 (P3) ASCs and DFBs at 3,000/cm^2, respectively. After cells reached 90% confluence, 250 µM L-ascorbic acid phosphate (Sigma-Aldrich, St. Louis, MO, USA) was added to the culture medium for another 10 days. Then, the deposited ECMs were treated with 0.5% Triton X-100 containing 20 mM ammonium hydroxide for 5 minutes at 37°C to remove the cells. The dECMs were stored in PBS containing 100 U/ml penicillin, 100 µg/ml streptomycin, and 0.25 µg/ml fungizone until use.

Evaluation of cell proliferation

Cell doubling time: P3 ASCs expanded on PLs were plated on AECM, DECM, or PLs at a density of 3,000/cm^2 with growth medium. After 5 days of incubation, the cells (n = 4) were detached and counted using a hemocytometer. The ASCs harvested were termed AE4, DE4, and PL4. After counting, AE4, DE4, and PL4 were further plated on AECM, DECM, or PLs at a density of 3,000/cm^2 with growth medium. The harvested cells were subsequently counted and termed AE5, DE5, and PL5. The P5 ASCs were seeded again as before, harvested, counted, and termed AE6, DE6, and PL6.

EdU cell proliferation assay: P3 ASCs expanded on PLs were plated on AECM, DECM, or PLs at a density of 3,000/cm^2 with growth medium. After the cells reached 30%-40% confluence, 10 µM 5-ethynyl-2'-deoxyuridine (EdU) (Invitrogen) solution was applied and incubated for 12 hours in a 37°C humidified incubator with 5% CO_2. The cells were then detached, fixed, permeabilized, and stained with fluorescence Alexa 647. Subsequently, the EdU fluorescence was detected (n = 4) and analyzed by FACSCalibur (BD Biosciences, San Jose, CA, USA).

The data were further analyzed using Flowing Software 2.5.1 (Perttu Terho, University of Turku, Finland).

Stemness genes and transcription factor expression assay

PL-expanded P3 ASCs were further expanded on either PLs, DECM, or AECM for one passage; the expanded cells were termed PL4, DE4, and AE4. Expanded AE4, DE4, and PL4 ASCs were evaluated for stemness-related gene expression and transcription factors using real-time polymerase chain reaction (PCR). Total RNA (n = 4) was extracted from the expanded cells using TRIzol (Life Technologies, Carlsbad, CA, USA). Then, 2 µg mRNA was used to synthesize cDNA by reverse transcriptase using a High-Capacity cDNA Archive Kit (Applied Biosystems, Foster City, CA, USA). Real-time PCR was performed with the iCycler iQ™ Multicolor RT-PCR Detection System (Applied Biosystems). Stemness-related genes nanog homeobox (*NANOG*; Assay ID Hs02387400_g1), nestin (*NES*; Assay ID Hs00707120_s1), SRY-box 2 (*SOX2*; Assay ID Hs01053049_s1), runt-related transcription factor 2 (*RUNX2*; Assay ID Hs01047973_m1), peroxisome proliferator-activated receptor gamma (*PPARG*; Assay ID Hs01115513_m1), and SRY-box 9 (*SOX9*; Assay ID Hs01107818_m1) and the endogenous control gene glyceraldehyde-3-phosphate dehydrogenase (*GAPDH*; Assay ID Hs04420632_g1) were selected for Custom TaqMan® Gene Expression Assays from Applied Biosystems. Relative transcript levels were calculated by the comparative Ct method ($\chi = 2^{-\Delta\Delta Ct}$, in which $\Delta\Delta Ct = \Delta E - \Delta C$, $\Delta E = Ct_{exp} - Ct_{GAPDH}$, and $\Delta C = Ct_{ct1} - Ct_{GAPDH}$).

Flow cytometry analysis

The MSC surface markers of AE4, DE4, and PL4 ASCs were measured by flow cytometry. The following primary antibodies conjugated with fluorescent labels were applied: CD73 (Abcam, Cambridge, MA, USA), CD90 (BD Pharmingen, San Jose, CA, USA), CD105 (Abcam), CD146 (Abcam), and stage-specific embryonic antigen 4 (SSEA4) (Abcam). The cell samples (n = 4) containing 3×10^5 cells were incubated with the above antibodies in darkness for 30 minutes. Then, fluorescence was detected and analyzed by FACSCalibur (BD Biosciences). Data were further analyzed using Flowing Software 2.5.1 (Perttu Terho).

Chondrogenic induction and evaluation

Chondrogenic induction: P3 ASCs expanded on PLs were further expanded on AECM, DECM, or PLs for one passage. The expanded ASCs were termed AE4, DE4, and PL4. Expanded cells (3.0 × 10^5) of AE4, DE4, and PL4 were centrifuged at 300 *g* in a 15-ml polypropylene tube for 7 minutes to form a pellet. After 24-h incubation (day 0), the pellets were cultured in serum-free medium containing high-glucose Dulbecco's modified Eagle's medium, 0.1 mM ascorbic acid-2-phosphate, 40 µg/ml proline, 100 nM dexamethasone, 1 × ITS™ premix (BD Biosciences; 6.25 µg/ml insulin, 6.25 µg/ml transferrin, 6.25 µg/ml selenous acid, 5.35 µg/ml linoleic acid, and 1.25 µg/ml bovine serum), 100 U/ml penicillin, 100 µg/ml streptomycin, 0.25 µg/ml fungizone, 10 ng/ml recombinant human transforming growth factor beta3 (TGF-β3; PeproTech, Inc., Rocky Hill, NJ, USA), and 10 ng/ml recombinant human bone morphogenic protein 6 (BMP6; PeproTech, Inc.) in a 37°C humidified incubator with 5% CO_2 and 5% O_2 for up to 28 days.

Real-time PCR for chondrogenic marker genes: Chondrogenesis-related genes SRY-box 9 (*SOX9*; Assay ID Hs01107818_m1), aggrecan (*ACAN*; Assay ID Hs00153936_m1), collagen type II alpha 1 chain (*COL2A1*; Assay ID Hs01060-322_g1), collagen type X alpha 1 chain (*COL10A1*; Assay ID Hs00950955_g1), and matrix metallopeptidase 13 (*MMP13*; Assay ID Hs00-942586_m1) and endogenous control gene *GAPDH* were selected for Custom Taqman® Gene Expression Assays from Applied Biosystems. Total RNA (n = 4) was extracted from pellets of day 0 and day 28 using an RNase-free pestle, and other real-time PCR procedures were conducted as described in 2.4.

Biochemical analysis of DNA and glycosaminoglycan (GAG) content: Representative pellets (n = 4) of both day 0 and day 28 were digested in PBE buffer (10 mM ethylenediaminetetraacetic acid and 100 mM phosphate, pH 6.5) containing 125 µg/ml papain and 10 mM cysteine. The amount of DNA was measured using the QuantiT™ PicoGreen® dsDNA assay kit (Life Technologies). The GAG content was measured using dimethylmethylene blue dye (Thermo Fisher Scientific, Waltham, MA, USA), and bovine chondroitin sulfate (Sigma-Aldrich) was used as a standard. Levels of DNA and GAG were de-

tected by a microplate reader (Varioskan™ LUX, Thermo Fisher Scientific).

Histological analysis: Representative pellets (n = 4) were harvested and fixed in 4% paraformaldehyde overnight. Then, the pellets were dehydrated in a gradient ethanol series, cleared with xylene, embedded in paraffin, and cut into 5-μm sections. Alcian blue and Safranin O staining were applied to detect sulfated GAGs.

Adipogenic induction and evaluation

Adipogenic induction: Expanded cells of AE4, DE4, and PL4 were seeded onto PLs at a density of 8,000/cm^2. When cells reached 90% confluence, they were cultured with adipogenic medium consisting of α-minimum essential medium, 10% fetal bovine serum, 1 μM dexamethasone, 10 μM insulin, 0.5 mM 3-isobutyl-1-methylxanthine, 200 μM indomethacin, 100 U/ml penicillin, 100 μg/ml streptomycin, and 0.25 μg/ml fungizone in a 37°C humidified incubator with 5% CO_2 for up to 12 days.

Real-time PCR for adipogenic marker genes: Adipogenesis-related genes peroxisome proliferator activated receptor gamma (*PPARG*; Assay ID Hs01115513_m1), CCAAT enhancer binding protein alpha (*CEBPA*; Assay ID Hs00-269972_s1), lipoprotein lipase (*LPL*; Assay ID Hs00173425_m1), adiponectin, and C1Q and collagen domain-containing (*ADIPOQ*; Assay ID Hs01060322_g1) and endogenous control gene *GAPDH* were selected for Custom Taqman® Gene Expression Assays from Applied Biosystems. Total RNA (n = 4) was extracted from induced cells, and real-time PCR procedures were conducted as described in 2.4.

Western blotting: Adipogenesis-induced cell samples were lysed in lysis buffer with protease inhibitors (Cell Signaling Technology, Danvers, MA, USA). Total protein was quantified using the BCA™ protein assay kit (Thermo Fisher Scientific). Twenty micrograms of protein was denatured and separated using a 12% polyacrylamide gel (Invitrogen) at 120 V for 2 hours at 4°C. The proteins were then transferred to a nitrocellulose membrane at 30 V and 4°C overnight. Membranes were blocked with 5% nonfat milk in Tris-buffered saline (TBS) and probed with primary adiponectin monoclonal antibody (MA1-054, Thermo Fisher Scientific) for 1 hour. The blot was washed with TBS containing 0.1%

Tween20 and further incubated with the appropriate horseradish peroxidase (HRP)-conjugated secondary antibody (RK244131, Thermo Fisher Scientific) for 1 hour. The blot was developed with a chemiluminescence kit (GE Healthcare, Chicago, IL, USA) and imaged using a GE gel documentation. An anti-β-actin antibody (Invitrogen) was used to normalize expression data and ensure equal loading.

Histological analysis: Induced cells in culture flasks were fixed with 4% paraformaldehyde for 1 hour. Then, an Oil Red O kit (Sigma-Aldrich) was applied to stain lipids.

Osteogenic induction and evaluation

Osteogenic induction: Expanded cells of AE4, DE4, and PL4 were seeded onto PLs at a density of 8,000/cm^2. When cells reached 90% confluence, they were cultured with osteogenic medium consisting of α-minimum essential medium, 10% fetal bovine serum, 100 U/ml penicillin, 100 μg/ml streptomycin, 0.25 μg/ml fungizone, 50 mg/l ascorbic acid-2-phosphate, 0.01 μM dexamethasone, and 10 mM β-glycerophosphate (Sigma-Aldrich) in a 37°C humidified incubator with 5% CO_2 for up to 21 days.

Real-time PCR for osteogenic marker genes: Osteogenesis-related genes runt-related transcription factor 2 (*RUNX2*; Assay ID Hs0104-7973_m1), bone gamma-carboxyglutamate protein (*BGLAP*; Assay ID Hs01587814_g1), Sp7 transcription factor (*SP7*; Assay ID Hs01866-874_s1), and secreted phosphoprotein 1 (*SP-P1*; Assay ID Hs00959010_m1) and endogenous control gene *GAPDH* were selected for Custom Taqman® Gene Expression Assays from Applied Biosystems. Total RNA (n = 4) was extracted from induced cells, and real-time PCR procedures were conducted as described in 2.4.

Western blotting: Osteogenically induced cell samples were collected and dissolved in cell lysis buffer. A primary osteocalcin monoclonal antibody (MA1-20788, Thermo Fisher Scientific) was applied for 1 hour, and further incubated with the horseradish peroxidase (HRP)-conjugated secondary antibody (RK244131, Thermo Fisher Scientific) for 1 hour. The blot was developed with a chemiluminescence kit (GE Healthcare, Chicago, IL, USA). An anti-β-actin antibody (Invitrogen) was used to normalize equal

loading. Other procedures were conducted as described in 2.7.3.

Histological analysis: Induced cells in culture flasks were fixed with 4% paraformaldehyde for 1 hour. Then, Alizarin Red solution (Sigma-Aldrich) was applied for 10 minutes to stain calcium nodules.

Statistical analysis

Numerical data are presented as the mean and standard deviation of the mean. The Mann-Whitney *U* test was applied for pairwise comparison. All statistical analyses were performed with SPSS 13.0 statistical software (SPSS Inc., Chicago, IL, USA). A *p* value less than 0.05 was considered statistically significant.

Results

dECM promoted ASC proliferation

The dECM prepared with DFBs and ASCs exhibited a similar appearance under a microscope (**Figure 1A**) and the flasks appeared to be coated with dense, randomly arranged matrix fibers. The ASCs seeded on PLs showed enlarged and flattened morphology, whereas on dECMs, they exhibited tiny spindle-like morphology (**Figure 1B**). The cells on dECMs grew following the random direction of the matrix fibers (**Figure 1B**). The topography of matrix fibers also provided a three-dimensional living space for the ASCs. Regarding the proliferative effect of dECMs, especially the AECM, the data of population doubling (PD) time from cell counting showed that ASCs expanded on both dECMs had a much shorter PD time compared with those expanded on PLs (**Figure 1C**). Furthermore, consistent with PD time results, EdU proliferation assay also showed that cell expansion on dECMs yielded a significant increase in DNA replication for a specific duration compared with cell expansion on conventional PLs (**Figure 1D**). Both the results of PD time and EdU proliferation assay proved that dECMs were much better expansion conditions than conventional PLs. However, the results also indicated that AECM had no better effect on the proliferation of ASCs than DECM.

Evaluation of stemness genes, transcription factors, and MSC surface markers

As ASCs are a kind of MSCs, we evaluated the effects of dECM expansion on ASCs stemness.

We tested three embryonic stemness genes (*NANOG*, *NES*, and *SOX2*), and AE4 showed significantly higher expression of *NANOG* than DE4 and PL4. Moreover, DE4 also expressed higher *NANOG* than PL4. However, none of the dECMs exhibited any superiority with regard to *NES* and *SOX2* (**Figure 2A**). For transcription factors, *SOX9*, *PPARG*, and *RUNX2* represented the potential of chondrogenesis, adipogenesis, and osteogenesis, respectively. AE4 showed a significant increase in all three transcription factor genes compared with DE4 and PL4. Moreover, DE4 expressed higher *SOX9* than PL4 (**Figure 2B**). Upregulation of transcription factors *SOX9*, *PPARG*, and *RUNX2* before differentiation induction suggested that AECM-mediated ASCs' expansion could modulate cell differentiation fate. Further analysis of MSC surface markers was done by flow cytometry. The data show that both CD146 and SSEA4 were upregulated by percentage and median in AE4. However, for CD73, CD90, and CD105, no differences in percentage were observed. AE4 showed a slight increase in the median of CD73 and a slight decrease in the median of CD105 (**Figure 2C**).

AECM promoted chondrogenic capacity of ASCs

To determine whether AECM expansion contributed to MSC potential maintenance, the chondrogenic, adipogenic, and osteogenic capacity of ASCs was evaluated after PL-expanded P3 ASCs were further expanded on PL, DE, and AE for one passage. The expanded ASCs were chondrogenically induced in a pellet culture system for 28 days. The pellets of AE4 were the largest, and those of PL4 were the smallest. The pellets were stained with Alcian blue and Safranin O to detect sulfated GAGs. The results demonstrated that AE4 pellets synthesized significantly more sulfated GAGs than PL4 and DE4 (**Figure 3A**). Biochemical analysis of DNA and GAG content was performed to evaluate the matrix deposition of chondrogenesis. The biochemistry data demonstrated that AE4 yielded the highest cell viability during chondrogenesis. AE4 also produced the highest amount of GAG per pellet and chondrogenic index (ratio of GAG to DNA) followed by DE4 and PL4, with the lowest (**Figure 3B**). The AE4 pellets showed the highest expression level of chondrogenic marker genes (*SOX9*, *ACAN*, and *COL2A1*) followed by those of DE4; the PL4 pellets showed the lowest level. With regard to hypertrophic markers (*COL10A1* and *MMP13*) of chondro-
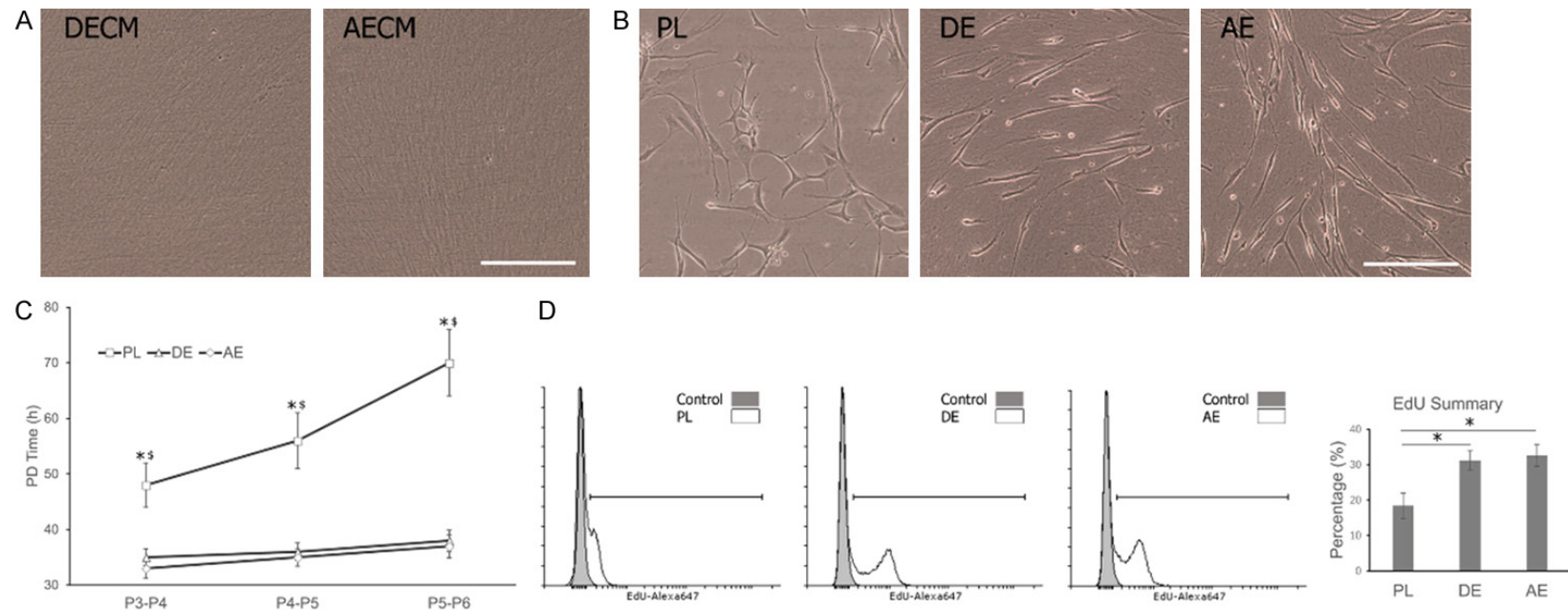
Figure 1. ECM enhanced proliferation of ASCs. A. Surface topography of dECMs prepared with DFBs (DECM) and ASCs (AECM) (scale bar: 400 µm). B. Cell morphology of passage 4 ASCs expanded on plastic flasks (PL), DECM (DE), and AECM (AE) (scale bar: 400 µm). C. Cell population doubling time calculated by cell counting from passage 3 to passage 6. Data are shown as the mean ± SD (n = 4). *means $P < 0.05$ between AE and PL, $means $P < 0.05$ between DE and PL, and $P < 0.05$ suggests statistically significant differences. D. Cell proliferation rate measured by EdU assay. Data are shown as the mean ± SD (n = 4). *means $P < 0.05$ suggesting statistically significant differences.
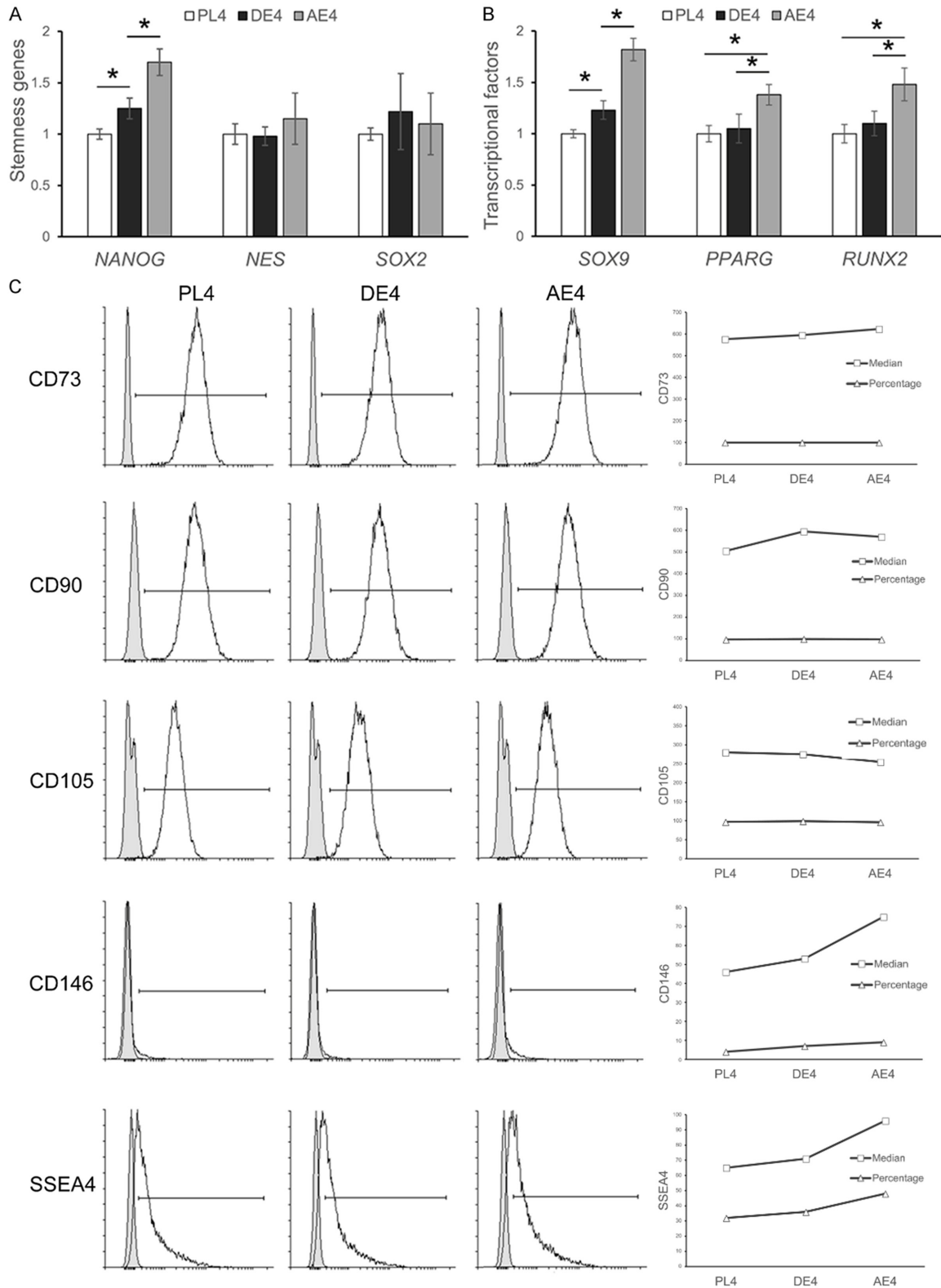
Figure 2. AECM-expanded ASCs exhibited increased expression of transcription factors. PL-expanded P3 ASCs were further expanded on either PLs, DECM, or AECM for one passage; the expanded cells were termed PL4, DE4, and AE4. A. Expression of stemness-related genes (*NANOG*, *NES*, and *SOX2*) in PL4, DE4, and AE4. B. Expression of transcription factors in PL4, DE4, and AE4. *SOX9*, *PPARG*, and *RUNX2* represent chondrogenesis, adipogenesis, and osteogenesis, respectively. C. Both the percentage and median of MSC surface markers (CD73, CD90, CD105, CD146, and SSEA4) were measured by flow cytometry of PL4, DE4, and AE4. Data are shown as the mean ± SD (n = 4). *means *P* < 0.05 suggesting statistically significant differences.
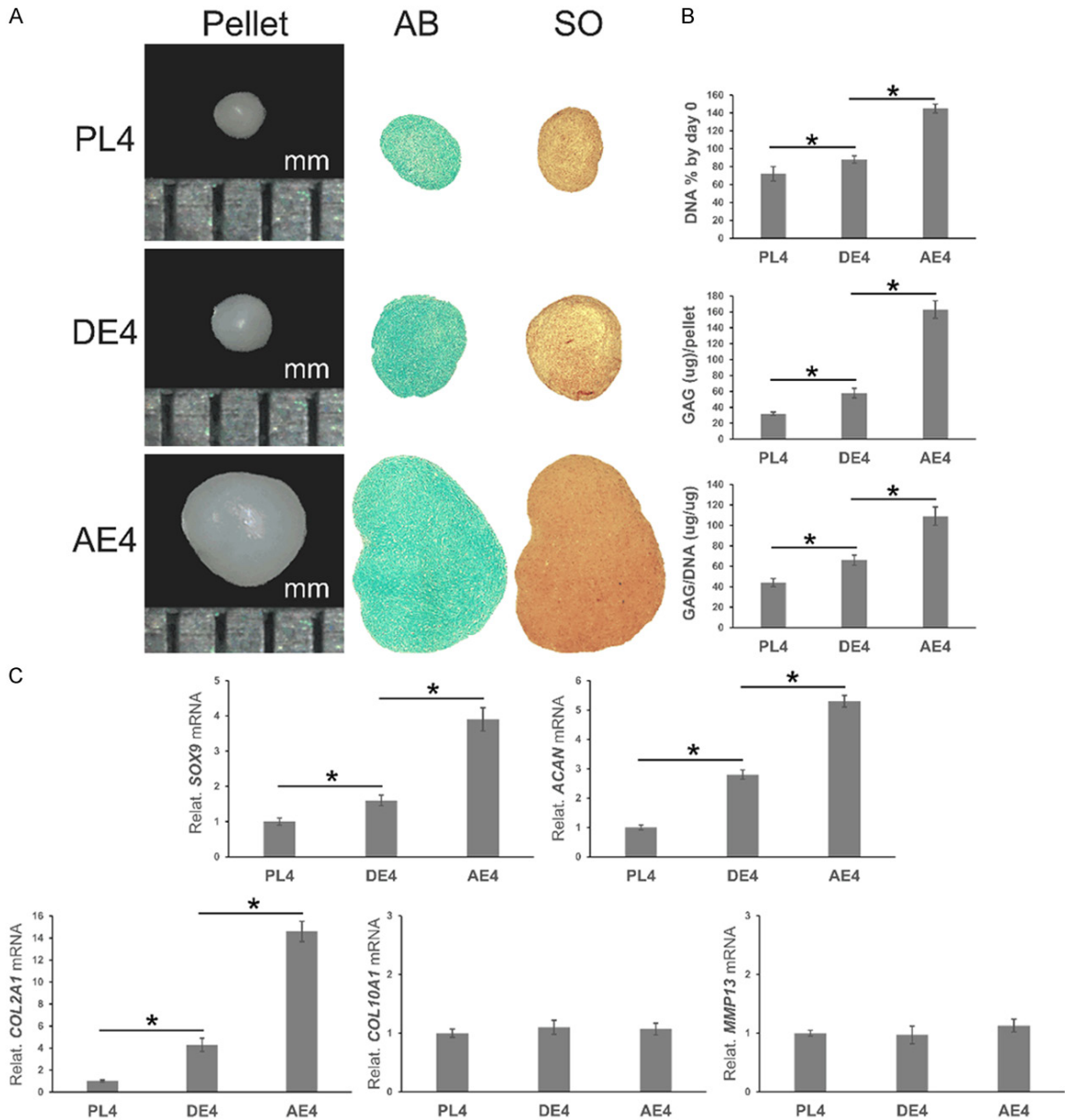
Figure 3. AECM promoted the chondrogenic capacity of ASCs. PL-expanded P3 ASCs were further expanded on either PLs, DECM, or AECM for one passage and the expanded cells were termed PL4, DE4, and AE4. PL4, DE4, and AE4 ASCs were chondrogenically induced by a pellet culture system for 28 days. A. Representative pellets were measured by a scale bar (mm) and histologically stained with Alcian blue (AB) and Safranin O (SO) to measure sulfated GAGs. B. Biochemical analysis of DNA and GAG content of representative pellets (n = 4). The DNA ratio (day 28 DNA content adjusted by day 0 content) was used to evaluate cell viability during chondrogenic induction; GAG content indicated matrix deposition of pellets, and the GAG/DNA ratio indicated chondrogenic index. C. Chondrogenic marker genes (*SOX9*, *ACAN*, and *COL2A1*) and hypertrophic marker genes (*COL10A1* and *MMP13*) during chondrogenic induction were evaluated by real-time PCR. Data are shown as the mean ± SD (n = 4). *means *P* < 0.05 suggesting statistically significant differences.

genesis, no statistical differences were observed among groups (**Figure 3C**).

AECM promoted adipogenic capacity of ASCs

The expanded ASCs of PL4, DE4, and AE4 were adipogenically induced for 12 days *in vitro*. AS-

Cs expanded on AECM exhibited more positive staining for Oil Red O than those expanded on DECM and PLs (**Figure 4A**). AE4 also showed higher expression of adipogenic marker genes (*PPARG*, *CEBPA*, and *ADIPOQ*) (**Figure 4B**) and synthesized more adipogenic marker protein (adiponectin) than DE4 and PL4 (**Figure 4C**); in
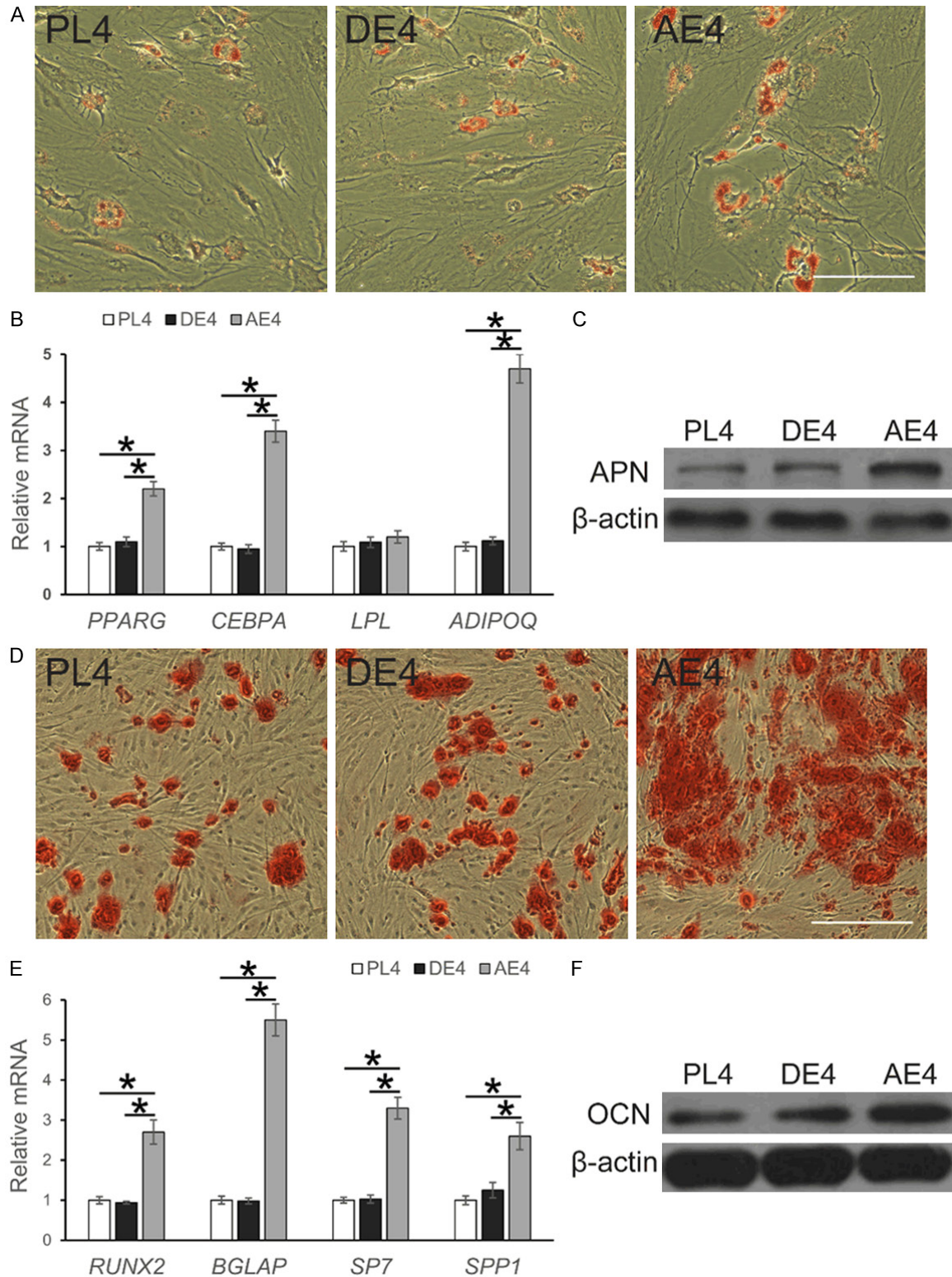
Figure 4. AECM enhanced the adipogenic and osteogenic differentiation of ASCs. PL-expanded P3 ASCs were further expanded on either PLs, DECM, or AECM for one passage and the expanded cells were termed PL4, DE4, and AE4. PL4, DE4, and AE4 ASCs were either adipogenically induced for 12 days or osteogenically induced for 21 days. A. Adipogenesis was evaluated by Oil Red O staining (scale bar: 400 μm). B. Expression of adipogenic marker genes (*PPARG*, *CEBPA*, *LPL*, and *ADIPOQ*) was measured by real-time PCR. C. Adiponectin (APN) level was evaluated by Western blot; β-actin was used to ensure equal loading. D. Osteogenesis was evaluated by Alizarin Red staining

(scale bar: 400 μm). E. Expression of osteogenic marker genes (*RUNX2*, *BGLAP*, *SP7*, and *SPP1*) was measured by real-time PCR. F. Osteocalcin (OCN) level was evaluated by Western blot; β-actin was used to ensure equal loading. Data are shown as the mean ± SD (n = 4). *means $P < 0.05$ suggesting statistically significant differences.

comparison of DE4 and PL4, no statistical differences in these markers were observed.

AECM promoted osteogenic capacity of ASCs

The expanded ASCs of PL4, DE4, and AE4 were osteogenically induced for 21 days *in vitro*. ASCs exapnded on AECM exhibited more positive staining for Alizarin Red than those expanded on DECM and PLs (**Figure 4D**). AE4 also showed higher expression of osteogenic marker genes (*RUNX2*, *BGLAP*, *SP7*, and *SPP1*) (**Figure 4E**) and synthesized more osteogenic marker protein (osteocalcin) than DE4 and PL4 (**Figure 4F**) in comparison of DE4 and PL4, no statistical differences in these markers were observed.

Discussion

Cell aging is a crucial problem in the current MSC-based bedside clinical therapies and trials [8, 16]. All MSCs can only expand for a limited time *in vitro* before senescence. The senescent state of MSCs leads to some apparent changes including proliferation arrest, size increase, phenotype change, and differentiation potential loss [8, 17]. It is believed that intrinsic factors such as DNA telomere shortening during replication and continuous global gene expression profile changes-especially a series of downregulation related to cell cycle, mitosis, and DNA repair-are determinants of senescence [18, 19]. However, the environmental conditions during *in vitro* cell expansion also play a considerable role. Conboy et al. [20] demonstrated that exposure to a young systemic environment could rejuvenate aged progenitor cells. Studies have also demonstrated that certain culture environments including culture cell-derived ECM and supplementation with cytokines can profoundly influence cell behaviors [13, 21]. ECM deposited by human bone marrow stromal cells could facilitate the proliferation and tissue-specific lineage potential of MSCs [22]. In addition, a young environment created by fetal MSCs-derived ECM could better rejuvenate MSCs potential than adult MSCs [12]. These studies suggested that optimizing the *in vitro* expansion environment is fundamental to MSCs applications and may

abate or even reverse the trend of senescence.

In this study, it was determined whether dECM from ASCs had an appreciable effect on ASCs' potential maintenance. dECM from DFBs and conventional PLs as controls was used. The results suggested that ASCs expanded on AECM yielded more successful chondrogenesis, adipogenesis, and osteogenesis along differentiation induction than those expanded on DECM or PLs. In terms of proliferation, both the AECM and DECM could considerably boost the self-renewal of ASCs.

In the cell proliferation assay, ASCs' PD time increased rapidly with passaging under conventional PL expansion. This phenomenon demonstrated that ASCs lost their self-renewal capacity quickly under conventional culture, which was consistent with previous reports [5, 16]. Interestingly, in both AECM and DECM expansion, the ASCs' PD time only slightly increased, proving that ECM expansion could successfully maintain the proliferative capacity of ASCs.

With regard to surface phenotype, increased expression of CD146 and SSEA4 was noted in AECM-expanded ASCs. CD146 is a marker for not only perivascular cells but also MSCs [23], and an increase in its expression may be linked to higher differentiation potential, especially chondrogenic potential [24-26]. SSEA4 is commonly used to define embryonic stem cells, and its role in adult MSCs may be related to differentiation potential [27]. Increased expression of SSEA4 here may suggest elevated differentiation potential by AECM expansion. In the evaluation of stemness gene expression, *NES* and *SOX2* did not exhibit any differences from each other. Interestingly, *NANOG* showed a differential expression pattern among the three expansion systems. *NANOG* is a critical transcription factor for maintenance of pluripotency in embryonic stem cells [28]. Recent studies demonstrated that ectopic Nanog could suppress senescence of fibroblasts [29] and reverse aged MSCs proliferation and myogenic potential [30, 31]. In this study, *NANOG* expression increased with ECM expansion, especially in AECM expansion, suggesting that the ECM

may maintain cell potential via upregulating *NANOG* expression.

A recent study showed that fibroblast-derived ECM could induce chondrogenic differentiation of ASCs [32]. Our study produced a consistent result, revealing that the ECM from DFBs could promote chondrogenic differentiation of ASCs. In addition, AECM had a better effect on chondrogenesis than DECM. Despite the chondrogenesis improvement, the ECM did not significantly increase expression of the hypertrophic pathway and related genes *MMP13* and *COL10A1* showed no differences between PLs and ECM culture. Usually, adipogenesis and osteogenesis are considered opposite physiological processes during differentiation determination; when one is increased, the other is decreased [33]. In this study, both adipogenesis and osteogenesis were promoted by the AECM. This could be because the overall potential of differentiation was improved by the AECM. Thus, chondrogenesis, adipogenesis, and osteogenesis were all improved.

In conclusion, AECM could facilitate cell proliferation and differentiation, representing a promising *in vitro* expansion system to maintain the self-renewal and differentiation potential of ASCs. From this expansion system it could be inferred that the results apply to other MSCs which have vast industrial application prospects. However, despite the demonstrated improvement of the *in vitro* performance of ASCs by expansion on ECM, the underlying mechanism is still unknown. In future investigations, high-throughput RNA-sequencing techniques and proteomics will be applied to compare the matrisomes from ECMs of different origins. This may enhance the understanding of ECM from a much broader perspective.

Acknowledgements

Disclosure of conflict of interest

None.

Address correspondence to: Dr. Jiasheng Dong, Department of Plastic and Reconstructive Surgery, Shanghai Ninth People's Hospital Affiliated to Shanghai Jiao Tong University School of Medicine, Shanghai, China. E-mail: dongjiasheng_9y@hotmail.com

References

[1] Mizuno H, Tobita M and Uysal AC. Concise review: adipose-derived stem cells as a novel tool for future regenerative medicine. Stem Cells 2012; 30: 804-810.

[2] Bunnell BA, Flaat M, Gagliardi C, Patel B and Ripoll C. Adipose-derived stem cells: isolation, expansion and differentiation. Methods 2008; 45: 115-120.

[3] Ruiz JC, Ludlow JW, Sherwood S, Yu G, Wu X and Gimble JM. Differentiated human adipose-derived stem cells exhibit hepatogenic capability in vitro and in vivo. J Cell Physiol 2010; 225: 429-436.

[4] Zhao Y, Jiang H, Liu XW, Chen JT, Xiang LB and Zhou DP. Neurogenic differentiation from adipose-derived stem cells and application for autologous transplantation in spinal cord injury. Cell Tissue Bank 2015; 16: 335-342.

[5] De Francesco F, Ricci G, D'Andrea F, Nicoletti GF and Ferraro GA. Human adipose stem cells: from bench to bedside. Tissue Eng Part B Rev 2015; 21: 572-584.

[6] Wang CH, Wang TM, Young TH, Lai YK and Yen ML. The critical role of ECM proteins within the human MSC niche in endothelial differentiation. Biomaterials 2013; 34: 4223-4234.

[7] Baxter MA, Wynn RF, Jowitt SN, Wraith JE, Fairbairn LJ and Bellantuono I. Study of telomere length reveals rapid aging of human marrow stromal cells following in vitro expansion. Stem Cells 2004; 22: 675-682.

[8] Bonab MM, Alimoghaddam K, Talebian F, Ghaffari SH, Ghavamzadeh A and Nikbin B. Aging of mesenchymal stem cell in vitro. BMC Cell Biol 2006; 7: 14.

[9] Shakouri-Motlagh A, O'Connor AJ, Brennecke SP, Kalionis B and Heath DE. Native and solubilized decellularized extracellular matrix: a critical assessment of their potential for improving the expansion of mesenchymal stem cells. Acta Biomater 2017; 55: 1-12.

[10] Anasiz Y, Ozgul RK and Uckan-Cetinkaya D. A new chapter for mesenchymal stem cells: decellularized extracellular matrices. Stem Cell Rev 2017; 13: 587-597.

[11] Pei M, Zhang Y, Li J and Chen D. Antioxidation of decellularized stem cell matrix promotes human synovium-derived stem cell-based chondrogenesis. Stem Cells Dev 2013; 22: 889-900.

[12] Li J, Hansen KC, Zhang Y, Dong C, Dinu CZ, Dzieciatkowska M and Pei M. Rejuvenation of chondrogenic potential in a young stem cell microenvironment. Biomaterials 2014; 35: 642-653.

[13] Hoshiba T, Chen G, Endo C, Maruyama H, Wakui M, Nemoto E, Kawazoe N and Tanaka M.

Decellularized extracellular matrix as an in vitro model to study the comprehensive roles of the ecm in stem cell differentiation. Stem Cells Int 2016; 2016: 6397820.

[14] Zhang Y, Pizzute T, Li J, He F and Pei M. sb-203580 preconditioning recharges matrix-expanded human adult stem cells for chondrogenesis in an inflammatory environment - a feasible approach for autologous stem cell based osteoarthritic cartilage repair. Biomaterials 2015; 64: 88-97.

[15] Franco-Barraza J, Beacham DA, Amatangelo MD and Cukierman E. Preparation of extracellular matrices produced by cultured and primary fibroblasts. Curr Protoc Cell Biol 2016; 71: 10-19.

[16] Maredziak M, Marycz K, Tomaszewski KA, Kornicka K and Henry BM. The influence of aging on the regenerative potential of human adipose derived mesenchymal stem cells. Stem Cells Int 2016; 2016: 2152435.

[17] Sethe S, Scutt A and Stolzing A. Aging of mesenchymal stem cells. Ageing Res Rev 2006; 5: 91-116.

[18] Itahana K, Campisi J and Dimri GP. Mechanisms of cellular senescence in human and mouse cells. Biogerontology 2004; 5: 1-10.

[19] Wagner W, Horn P, Castoldi M, Diehlmann A, Bork S, Saffrich R, Benes V, Blake J, Pfister S, Eckstein V and Ho AD. Replicative senescence of mesenchymal stem cells: a continuous and organized process. PLoS One 2008; 3: e2213.

[20] Conboy IM, Conboy MJ, Wagers AJ, Girma ER, Weissman IL and Rando TA. Rejuvenation of aged progenitor cells by exposure to a young systemic environment. Nature 2005; 433: 760-764.

[21] Pizzute T, Li J, Zhang Y, Davis ME and Pei M. Fibroblast growth factor ligand dependent proliferation and chondrogenic differentiation of synovium-derived stem cells and concomitant adaptation of wnt/mitogen-activated protein kinase signals. Tissue Eng Part A 2016; 22: 1036-1046.

[22] Pei M, He F and Kish VL. Expansion on extracellular matrix deposited by human bone marrow stromal cells facilitates stem cell proliferation and tissue-specific lineage potential. Tissue Eng Part A 2011; 17: 3067-3076.

[23] Covas DT, Panepucci RA, Fontes AM, Silva WA Jr, Orellana MD, Freitas MC, Neder L, Santos AR, Peres LC, Jamur MC and Zago MA. Multipotent mesenchymal stromal cells obtained from diverse human tissues share functional properties and gene-expression profile with CD146+ perivascular cells and fibroblasts. Exp Hematol 2008; 36: 642-654.

[24] Russell KC, Phinney DG, Lacey MR, Barrilleaux BL, Meyertholen KE and O'Connor KC. In vitro high-capacity assay to quantify the clonal heterogeneity in trilineage potential of mesenchymal stem cells reveals a complex hierarchy of lineage commitment. Stem Cells 2010; 28: 788-798.

[25] Ulrich C, Abruzzese T, Maerz JK, Ruh M, Amend B, Benz K, Rolauffs B, Abele H, Hart ML and Aicher WK. Human placenta-derived CD146-positive mesenchymal stromal cells display a distinct osteogenic differentiation potential. Stem Cells Dev 2015; 24: 1558-1569.

[26] Su X, Zuo W, Wu Z, Chen J, Wu N, Ma P, Xia Z, Jiang C, Ye Z, Liu S, Liu J, Zhou G, Wan C and Qiu G. CD146 as a new marker for an increased chondroprogenitor cell sub-population in the later stages of osteoarthritis. J Orthop Res 2015; 33: 84-91.

[27] Katikireddy KR, Dana R and Jurkunas UV. Differentiation potential of limbal fibroblasts and bone marrow mesenchymal stem cells to corneal epithelial cells. Stem Cells 2014; 32: 717-729.

[28] Loh YH, Wu Q, Chew JL, Vega VB, Zhang W, Chen X, Bourque G, George J, Leong B, Liu J, Wong KY, Sung KW, Lee CW, Zhao XD, Chiu KP, Lipovich L, Kuznetsov VA, Robson P, Stanton LW, Wei CL, Ruan Y, Lim B and Ng HH. The Oct4 and Nanog transcription network regulates pluripotency in mouse embryonic stem cells. Nat Genet 2006; 38: 431-440.

[29] Munst B, Thier MC, Winnemoller D, Helfen M, Thummer RP and Edenhofer F. Nanog induces suppression of senescence through downregulation of p27KIP1 expression. J Cell Sci 2016; 129: 912-920.

[30] Han J, Mistriotis P, Lei P, Wang D, Liu S and Andreadis ST. Nanog reverses the effects of organismal aging on mesenchymal stem cell proliferation and myogenic differentiation potential. Stem Cells 2012; 30: 2746-2759.

[31] Mistriotis P, Bajpai VK, Wang X, Rong N, Shahini A, Asmani M, Liang MS, Wang J, Lei P, Liu S, Zhao R and Andreadis ST. NANOG reverses the myogenic differentiation potential of senescent stem cells by restoring ACTIN filamentous organization and SRF-dependent gene expression. Stem Cells 2017; 35: 207-221.

[32] Dzobo K, Turnley T, Wishart A, Rowe A, Kallmeyer K, van Vollenstee FA, Thomford NE, Dandara C, Chopera D, Pepper MS and Parker MI. Fibroblast-derived extracellular matrix induces chondrogenic differentiation in human adipose-derived mesenchymal stromal/stem cells in vitro. Int J Mol Sci 2016; 17: 1259.

[33] James AW. Review of signaling pathways governing MSC osteogenic and adipogenic differentiation. Scientifica (Cairo) 2013; 2013: 684736.